Directed Research II

Gas Plumes analysis using Multibeam EM710 Water Column Image in Saint John River

By

Hesham Elhegazy

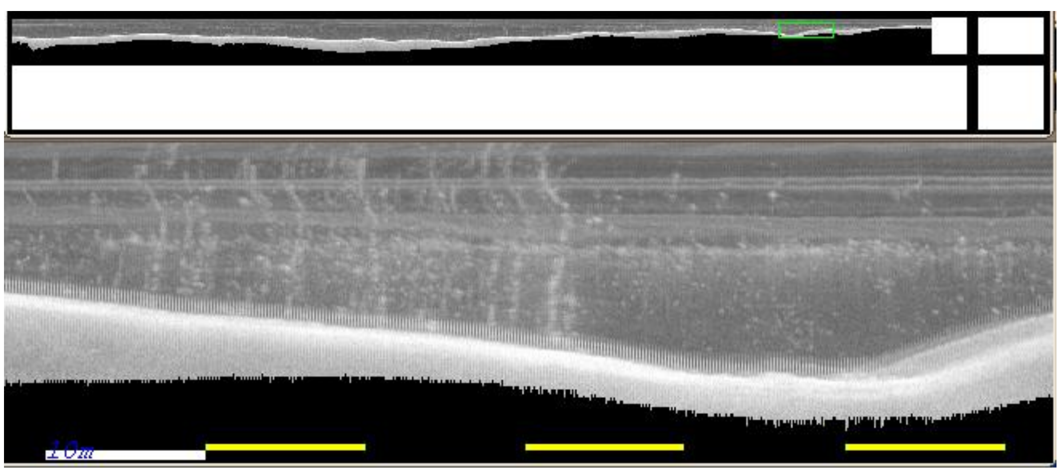

Supervisor:

Dr. John E. Hughes Clarke

September 6th, 2011

Contents

Table of Plots

1. Background of gas plumes

Gas plumes can be seen in oceans, seas, and rivers. The gas coming out is predominantly Methane gas (CH4). The gas released from the sea bed is affected by temperature which is the water temperature and the geothermal gradient, and also pressure which depends on water depth and depth beneath sea bed. (Westbrook, 2009)

Marine seeps contribute to atmospheric methane. They release gas as bubbles or oil and gas as oily bubbles or oil as droplets. There are two sources for marine seeps, biogenic which is the bacterial production of gas, and thermogenic which relates to subsurface petroleum reservoirs that leak to the surface.

Some seep gas arises from methane hydrate dissociation. For hundreds of years, people burned a lot of coal, oil and natural gas, but recently people started talking about methane hydrate as a future source for energy from the ocean because it contains methane gas which is the main component of natural gas.

The methane molecules are enclosed in microscopic cages composed of water molecules, which is called methane hydrates. It is a white ice-like solid that consist of methane and water.

The sea floor is a good place for the formation of methane hydrate because it is only stable under pressure of about 350 m and low temperature.

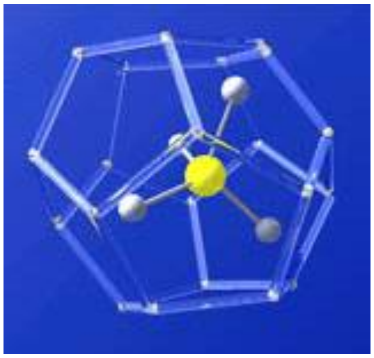

Figure 1: Methane hydrate, where methane molecules are captured in between water molecules (World ocean review)

Methane hydrate is created due to physical, chemical and geological conditions. The best condition is the presence of high water pressure and low temperature. If the water is warm, this will not prevent the creation of methane hydrate but there should be high water pressure to press the water molecule into a clathrate cage.

The sun heat worms the water surface, and the layers below it with a less degree. But the sun heat gets weaker as we go deeper in the water. Therefore the bottom water is cold with temperature between 0 - 4 degrees Celsius. But we have to put in mind that if depth is too deep, going down to the thick sediment layers on sea floor, the temperature will start to get higher again because we get closer to the earth center which evolves heat. For example in depths greater than 1 km, the temperature rises to over than 30°c, therefore no methane hydrate can be formed.

Figure 2: Methane hydrate obtained from the sea floor during a research expedition off the coast of Oregon (World ocean review)

Methane gas originally created from microorganisms which lives in deep sediment layers and slowly converts organic substances to methane, these organic materials are the remains of plankton that lived in the ocean long time ago, sank to the ocean floor and were finally in corporate into the sediments.

Methane gas is transferred from the sea bed to sea surface in the shape of bubbles that exchange gas with the surrounding aqueous environment.

Figure 3: Methane Bubbles going up to the Surface of an Arctic Lake (Ref.: http://www.youtube.com/watch?v=eM5WPl69Z18)

We are interested in methane seeps because it is a potential energy source that gives preliminary measurements of high flow rates and methane concentration. Also for their contribution in the global budgets, where on the climate change side, quantifying natural seeps to atmospheric CH4 sources may change our understanding of the global balance between human and natural sources. Therefore the big interest in methane is that it is a future energy source and also for preventing climate risk.

Factors affecting the marine seep gas:

After bubbles are formed and it starts to take its way from the sea floor up through the water to reach the surface of the water, during this trip, the marine seep bubble will end in one of three cases:

1. Dissolves in deep sea water, and in this case it will not affect the atmospheric budget, but provides energy source for deep sea ecosystem.

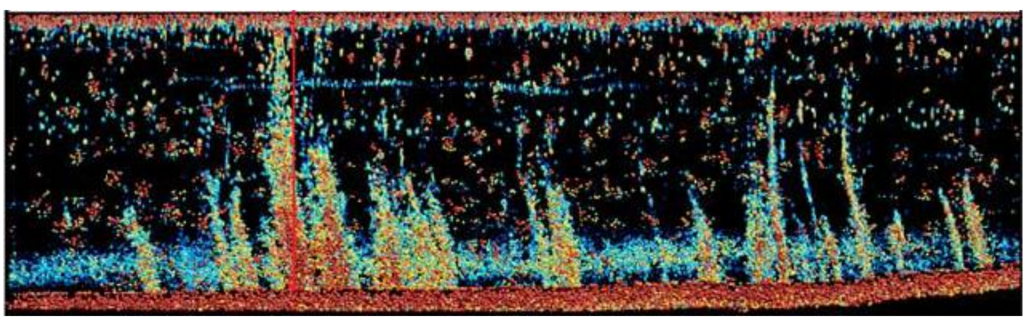

Figure 4: Gas bubbles coming out from the sea bed at West Spitsbergen (Ref. http://www.ecoseed.org/technology/science/article/29-science/4006-global-warming--methane-gas-found-rising-from-seabed-at-west-spitsbergen)

2. Transport to the surface mixed layer, and in this case methane contributes to global atmospheric budget. When bubbles dissolve in a mixed layer, some fraction of the

methane dissolved into the mixed layer can transfer to the atmosphere by air-sea gas exchange.

3. Transport to the sea surface and then to the atmosphere.

Figure 5: Methane Bubbles to the Surface of an Arctic Lake (Ref.: http://www.youtube.com/watch?v=eM5WPl69Z18)

Bubble speed:

An experiment was done by Peter G. Brewer to calculate the rise rate and dissolution rate of freely released CO2 droplet in the open ocean. The initial rise rate for 0.9-cm diameter droplet was 10cm/s at 800m. The droplet ascent from 800m to 340m depth over a period of about 1 hour which means a mean rise rate of 12.8 cm/sec. In another trial, the mean rise rate was 12.4 cm/sec, and this was due to a measurable increase in velocity with decreasing pressure and diminishing size; the initial rise rate was 10.2 cm/sec increasing gradually to 14.9 cm/sec at depths shallower than 450 meter.

Acceleration is assumed to be instantaneous and the upward velocity is determined by the spherical buoyancy equation:

$$U = [8gr\,(\rho sw - \rho CO2/\,(3\,\rho_{co2})]^{0.5}$$

Where assuming a drag coefficient of 1, U is the terminal rise velocity for a rigid sphere, g is the acceleration of gravity, r is the droplet/sphere radius and ρsw and $\rho CO2$ are the changing in situ densities of seawater and liquid CO_2, respectively. (Peter G. Brewer et al 2002)

2. Method used: EM710 Water Column Imaging

Since the beginning of the Millennium, mapping the sea floor have seen remarkable advances in the ability to map rapidly and more accurate. Resolution of the sea floor mapping in both temporal and spatial was increased. The EM 710 can also provide acoustic returns from the water column as well as the sea floor.

Water column data can provide information about high standing objects in water like sunk ships masts and offer information about least depth detection. Also water column data provide information for fisheries research regarding qualitative descriptions of fish school behavior. Finally the ability to map the water column has great potential for quantifying the flux of methane into the water from natural or unnatural seeps. And it has the power to detect the gas bubbles coming out from the sea bed through the water column to the sea surface, which is the important characteristic for the water column tool for this research topic.

Characteristics of EM 710:

The EM 710 operates at sonar frequencies in the 70 to 100 kHz range. The transmit fan is divided into three sectors to maximize range capability but also to suppress interference from multiples of strong bottom echoes. The sectors are transmitted sequentially

within each ping, and uses distinct frequencies or waveforms.

Both CW pulses of different lengths and even longer, compressible waveforms (chirps) are utilized. The alongtrack beamwidth depends upon the chosen transducer configuration with 0.5, 1 and 2 degrees available as standard. Focusing is applied individually to each transmit sector to retain the angular resolution inside the near field. A ping rate of up to 25 per second is possible. The transmit fan is electronically stabilized for roll, pitch and yaw.

The EM 710 has a receive beamwidth of either 1 or 2 degrees depending on the chosen receive transducer. The number of beams is 256 or 128 respectively, with dynamic focusing employed in the near field.

A high density beam processing mode provides up to 400 or 200 soundings per swath by using a limited range window for the detections, which in practice is equivalent to synthetically sharpening the beamwidth.

With a 1° transmit and 2° receive transducer the system will be able to generate two separate along track swaths per ping. The system produces up to 800 soundings per ping in this mode. The beam spacing may be set to be either equiangular or equidistant. The receive beams are electronically roll stabilized.

This can be used to increase the resolution beyond what is achievable in normal operation. In high density mode, the size of each acoustic footprint is reduced to fit the higher sounding density. The coverage may be limited by the operator either in angle or in swath width without reducing the number of beams.

A combination of phase and amplitude bottom detection algorithm is used, in order to provide soundings with the best possible accuracy. (Product description, EM 710 Multibeam echo sounder – Kongsberg)

Water column imaging:

Water column imaging can be only applied to systems using narrow receive beams, the reason for this is that narrow receive beams use a methodology that relies on assuming a single angle solution at a given slant range (JHC,2006) which discriminate the angles relationship of multiple echoes that occurs at a fixed time. Other systems such as interferometric systems allow up to three solutions at a given slant range.

The images shown by using water column are either Time-Angle space or Depth across track space.

The Time-Angle space in which the echo intensity can be mapped in a two dimensional image with angle on one axis and time on the other, and we can see a flat sea floor as a parabolic trace.

The Depth across track space is mainly for topographic imaging, the echo intensity field has to be mapped into the approximately two dimensional near-vertical planes under the vessel. By doing this we have to transform polar coordinates to Cartesian. Complications in this transformation can occur due to irregular or uneven beam spacing. Refracted ray paths and the along track distortion of the transmit beam pattern due to pitch steering must also be taken into account. (JHC, 2006)

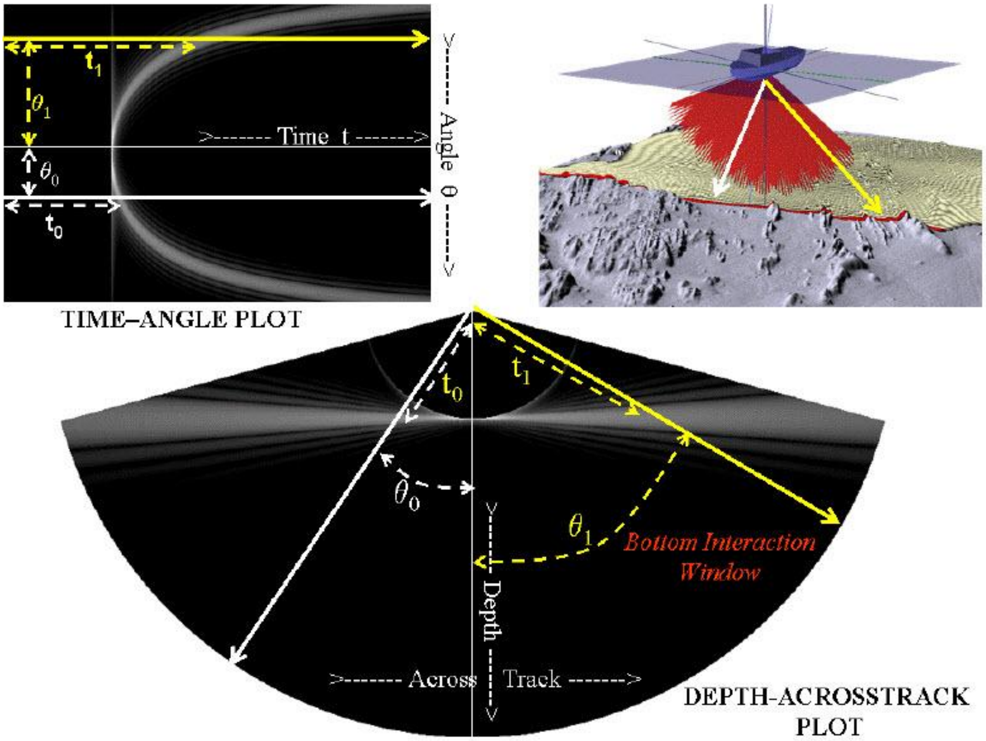

Figure 6: Time angle plot (Upper Left), Depth across Track plot (Lower) [JHC, 2006]

Understand the water column imagery:

The plot is constructed radially of time series along a specific beam azimuth in the EM 710, which is a Mills cross sonar, each beam has a mainlobe and sidelobes, and pattern –which is formed- is a result of the interaction between the main and sidelobes of the transmit beam and receiver channel for that beam. (JHC, 2006)

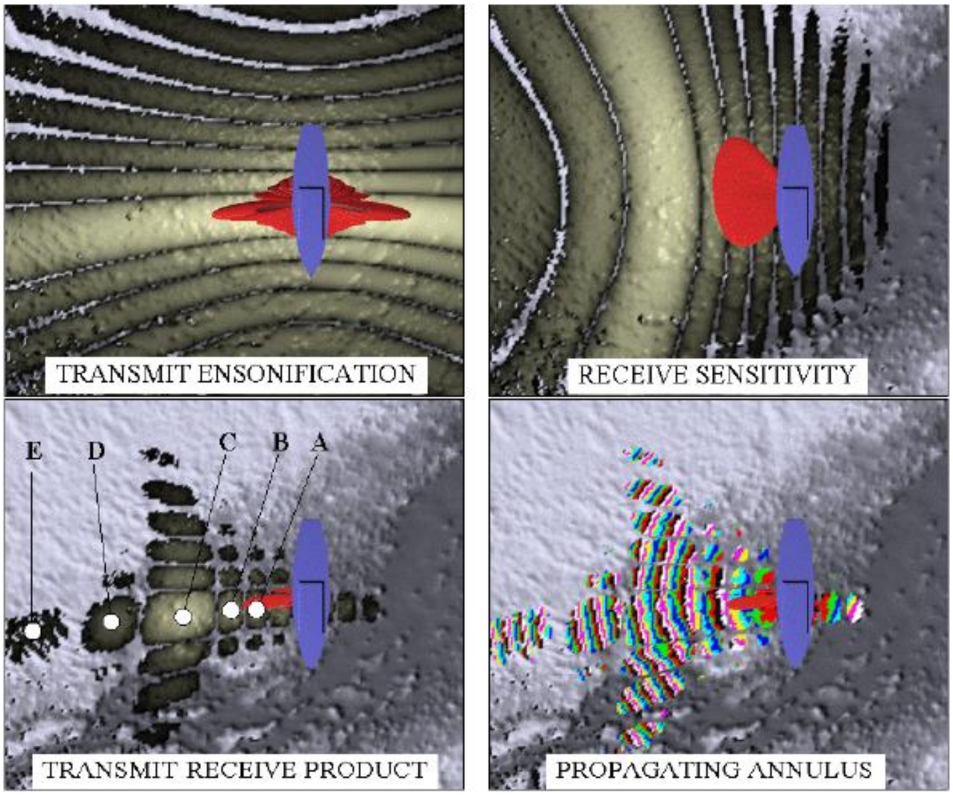

Figure 7: Illustrating the full transmits ensonification (top-left) and receiver sensitivity (top-right) pattern from single beam sonar. The resulting effective illumination pattern (bottom-left) and the way in which the outgoing pulse propagates through the beam footprint (bottom- right). [JHC, 2006]

Since we are concerned about the water column imagery, therefore we have to put in mind the pulse annulus propagation, which will give a series of echoes that will be received before and after the main echo. We have to realize that due to this, the beams away from nadir will pick up echoes inboard of the boresite, including the near first arrival, which will cause confusion when we are looking at the water column.

Because of the sidelobes, the seabed echoes will cause confusion in the water column data at any slant range more than the closest distance of approach to the seabed. Therefore in the water column tool in swathed software we have a semi circle option on the water column image that show us the best view for the water column image, where the best view will be within a semi-circle of radius equal to the minimum slant range to the seafloor as we can see in figure 9.

Two main things will control this confusion in the water column imagery:

1. The suppression of sidelobes.
2. Nature of the sea floor, which will affect the backscatter strength that changes with the grazing angle.

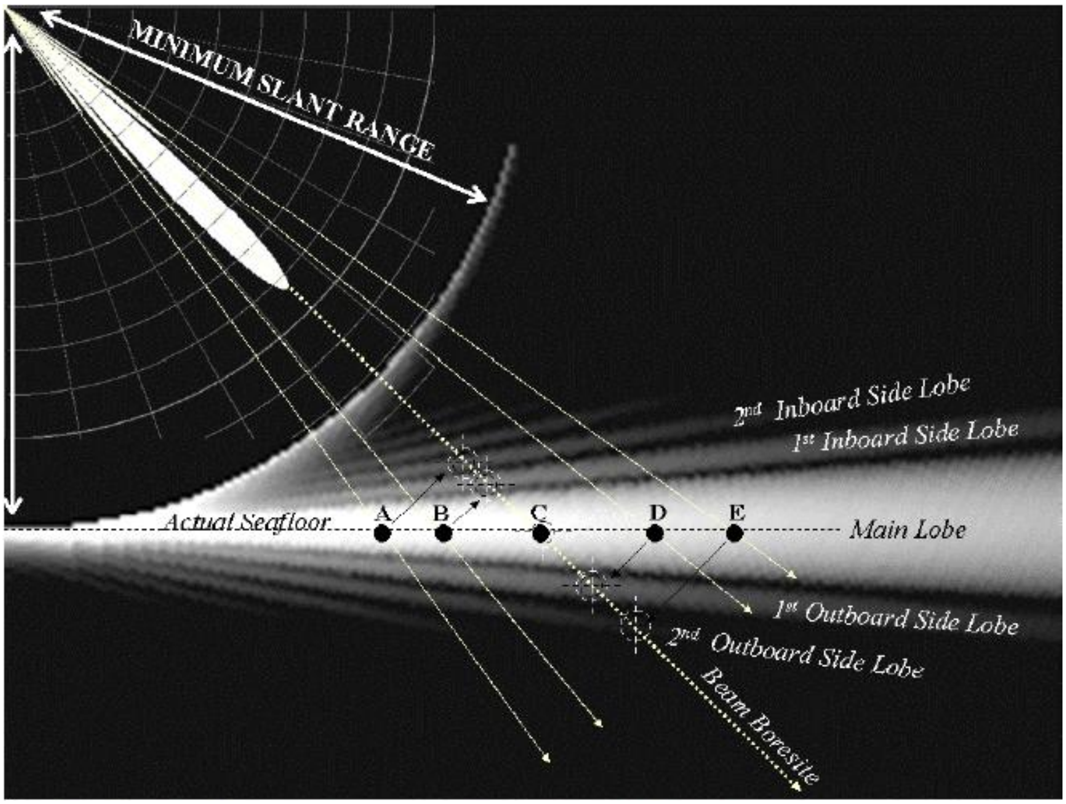

Figure 8: Subset of the polar plot display with receiver beam pattern superimposed. (JHC,2006)

3. Area of interest

Oceanography and Geology

The Kennebecasis Bay joins the estuary of the Saint John river towards its lower end, it goes from narrow to wide through a rocky gorge about 150 to 450 meter wide called The Reversing Falls into Saint John Harbor. In the central part of the Kennebecasis is a large island about 6.5km long and 1.5km wide that separates the bay into two channels.

The Kennebecasis Bay on the Saint John River is a 2-layer system with a brackish surface layer overlaying a deep saline layer. Two sills separate and restrict exchange of deep water in Kennebecasis Bay from that of the Bay of Fundy. (Trites, 1959)

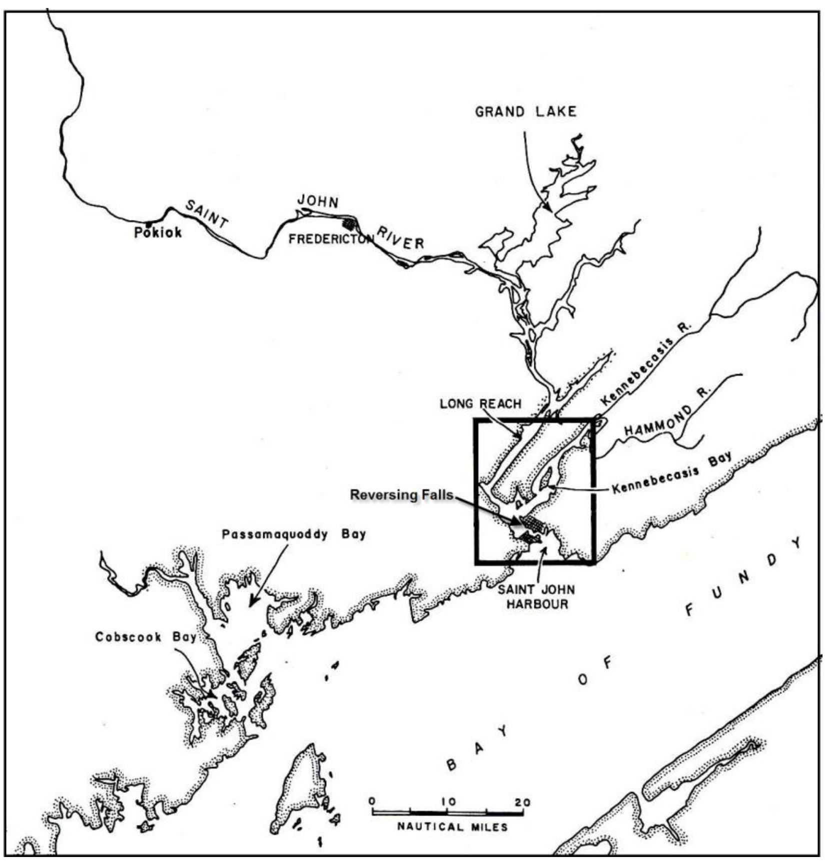

Figure 9: Kennebecasis Bay in relation to Saint John River and Bay of Fundy

The two sills are:

Reversing Falls Sill, located at the mouth of Saint John River, a 5 meters deep rock. This sill restricts the amount of fresh water that can pass from Saint John River to the Bay of Fundy and the amount of saline water that can pass from the Bay of Fundy to Saint John River.

The flow of water to either side is determined by the water level on either side of the sill. When normal water levels occur and the river is close to high tide, the water level on the seaward side of the sill tends to be higher than that of the river, therefore, sea water is able to flow upstream into the river. (Delpeche, 2007)

Grand Bay Sill, located approximately 6 km upstream of the Reversing Falls. The shallowest depth of the sill varies between 6m and 8.4m. (Hughes Clarke and Haigh, 2005)

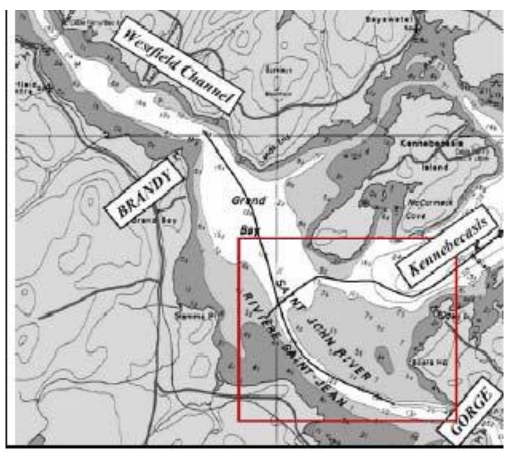

Figure 10: Boars Head Sill (Hughes Clarke and Haigh, 2005)

In between these two sills there is a place called the gorge area which acts as a mixing bowl for the saline water from the Bay of Fundy and the fresh water of the Saint John River.

During periods of Low River run off combined with spring tides a portion of the mixed water penetrates inward over the sill at the entrance of Kennebecasis Bay.

The depth of the fresh water layer in Kennebecasis Bay is controlled by the Saint John River outflow, and the sill at the Reversing Falls, rather than by the fresh water discharged directly into the Kennebecasis by the Hammond and Kennebecasis Rivers. The salinity of the deep layer remains relatively constant in Kennebecasis bay (21 to 23 ppt). Temperature of the deep layer may remain relatively constant for several months at a time, but varies within the range 2.5 to 12 degree Celsius. The dissolved oxygen concentration in the surface layer is usually at or near saturation values. The deep layer values in Kennebecasis Bay vary from approximately 30 to 50% saturation. Evidentially there is a high oxygen demand in this layer or a relatively sluggish circulation, or a combination of both. (Trites, 1959)

4. Experiment

In June 2010, the Ocean mapping group at UNB had their regular summer Hydrocamp using the research vessel CLS Heron. In this year the survey took place in the area of the Kennebecasis in Saint John River. The multibeam used during the survey was the EM 710, which has the ability to detect the water column. After we started the survey going out bound in the Kennebecasis bay, we realized bubbles in the water column in the first line.

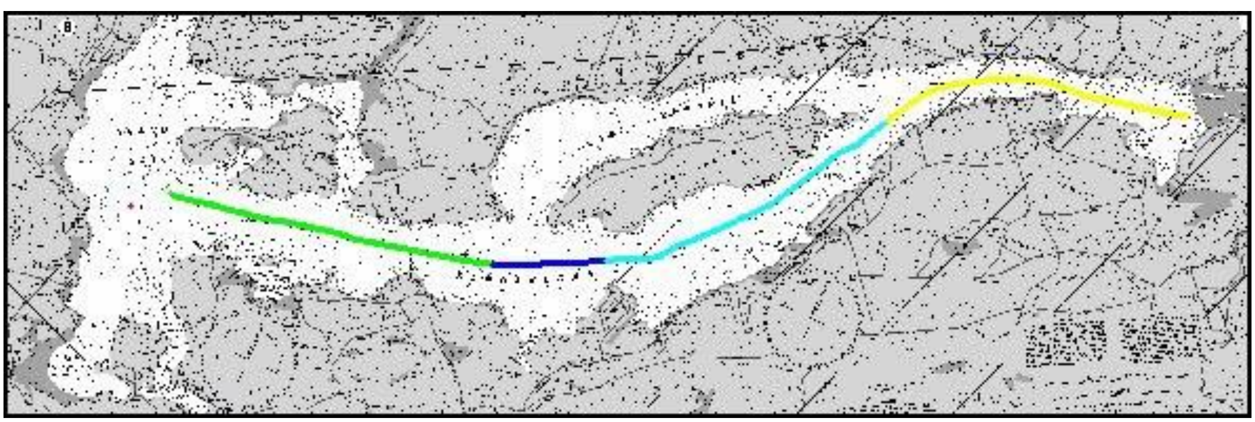

Figure 11: Line 1 (green)

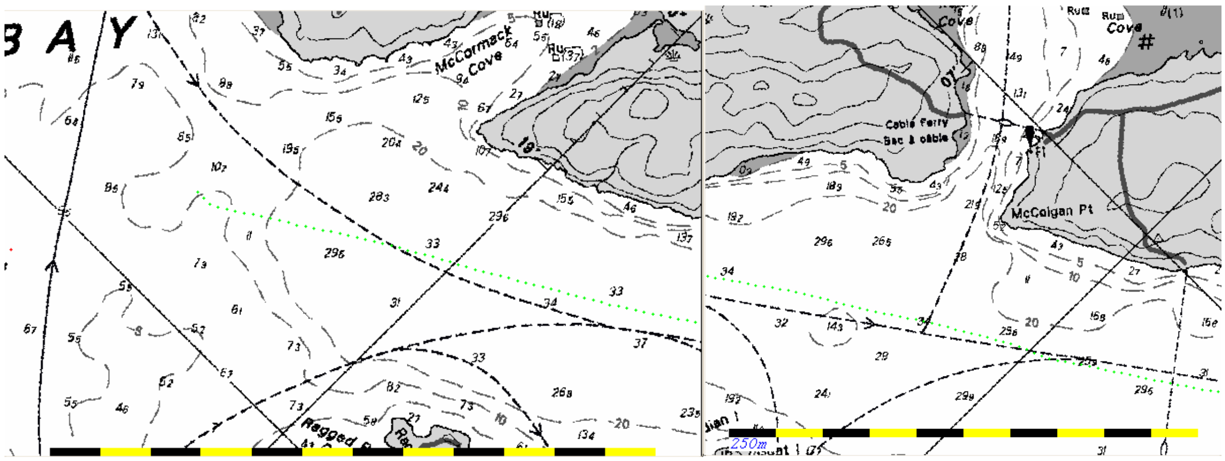

Figure 12: Subsets for line 1 where the bubbles were seen

In (Figure 14) we can see the results from UNB Hydrocamp 2010 for the subbottom for line one (the green line). The subbottom image shows the nature of the sea bed in the Kennebecasis Bay. The first part of the image is darker in color than the rest of the picture and also we can't see any details of the subbottom, which indicates the presence of gas in this area

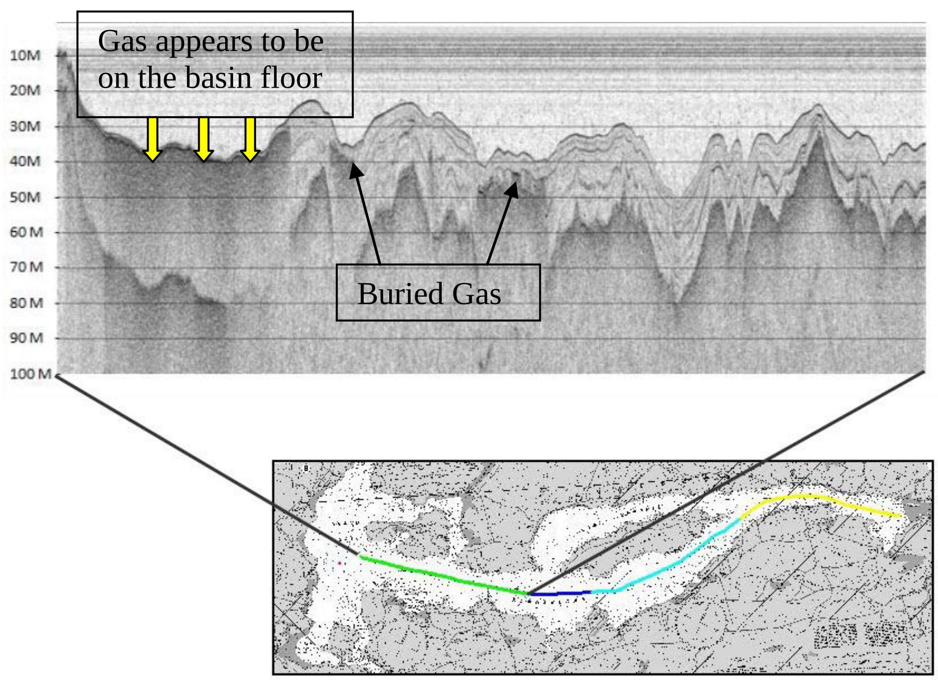

Figure 13: Subbottom for line 1(green)

We can see here under (Figures 16, 17 and 18) MVP results from UNB Hydrocamp 2010 for the lower channel of the Kennebecasis bay.

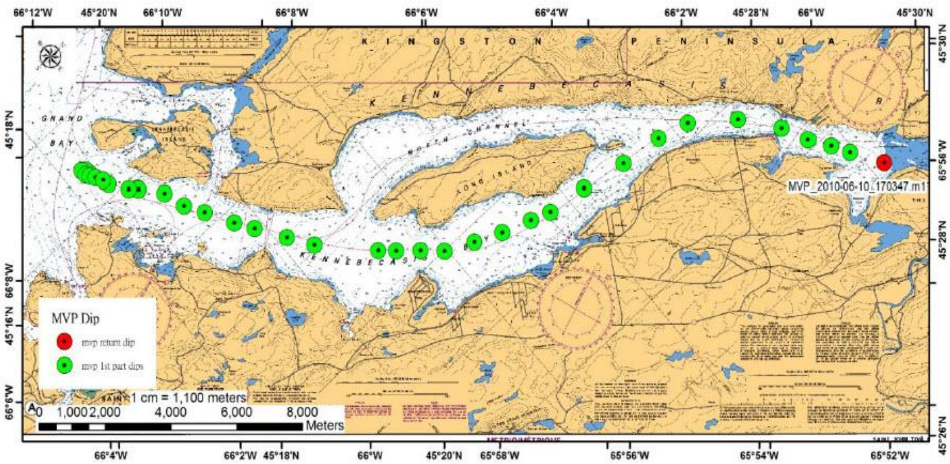

Figure 14: MVP's in the lower channel of Kennebecasis Bay

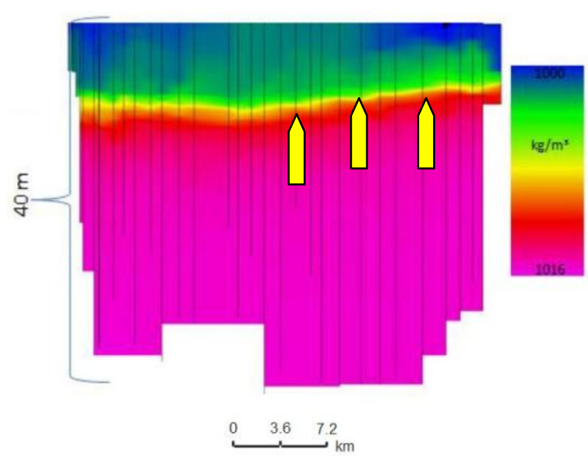

Figure 15: Yellow arrows shows Density level goes up towards NE

The Density image shows that heavy density is down, which is the salty water at the bottom of the channel, while less heavy density water is up which is fresh water.

Also the fact that this slopes up (where the yellow arrows are pointing) to the NE proves that the worm source of the fresh water is the Saint John River not the Hammond and Kennebecasis River.

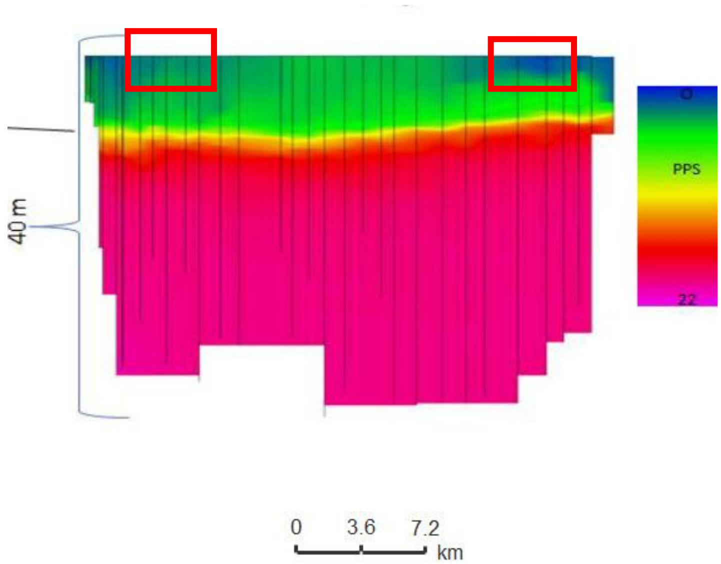

Figure 16: low Salinity in the upper corners (red rectangles) due to fresh water input

The salinity image tells us that the salty water is the lower layer in the channel and is about 21ppt while the fresh water is the upper layer of the channel.

The Blue color on the upper left of the image (left red rectangle) is a sign of fresh water injected from Saint John River, while the stronger blue color on the top right of the image (right red rectangle) is a sign of fresher water due to local input of the Hammond and Kennebecasis River.

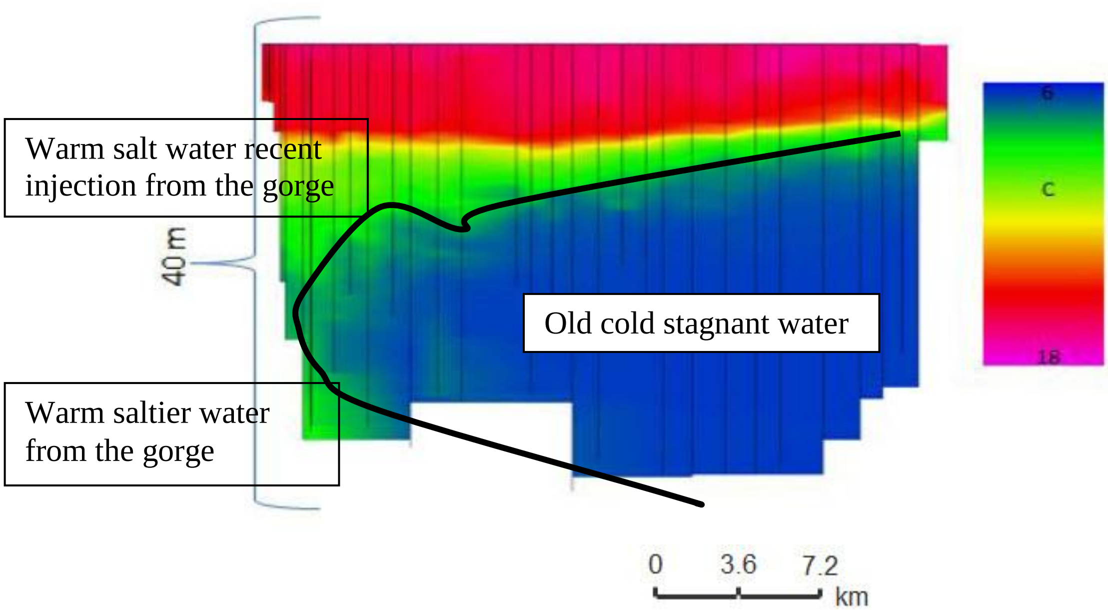

Figure 17: Temperature

From the temperature image we see that the warmer most recent injections of salt water from the gorge (green) is in the middle layer of the channel, and part of it is in the lower layer of the channel which is the salty water. Old cold water (blue) is in the lower layer of the channel. Using the EM 710 imagery collected at the same time as the MVP, it was clear that gas plumes are only present at the salt water end of the fjord above the subbottom gas evidence.

At the end of the survey we decided to do another two lines in this area at the entrance of the bay to determine exactly where the bubbles are coming out from. (Figure 18)

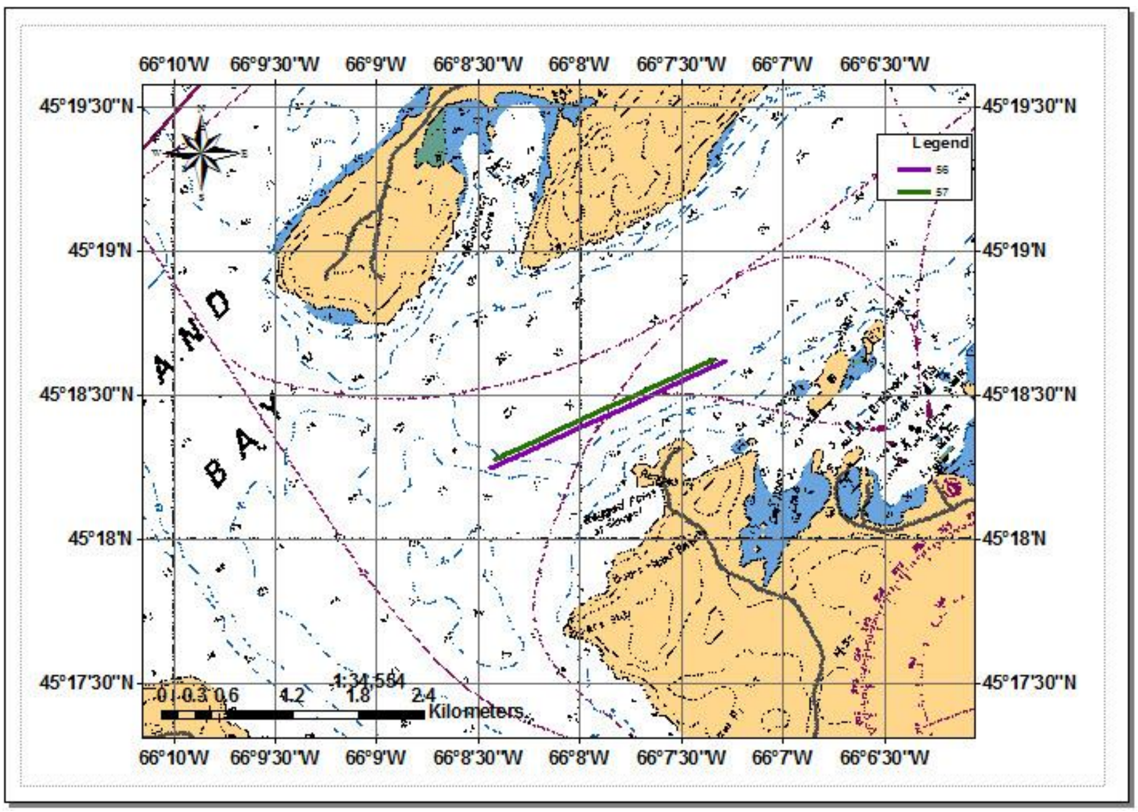

Figure 18: Two line in June survey to locate the gas plumes

In October 19th 2010, another bigger survey was done in the same area at the entrance of the Kennebecasis bay with 16 lines. (Figure 19)

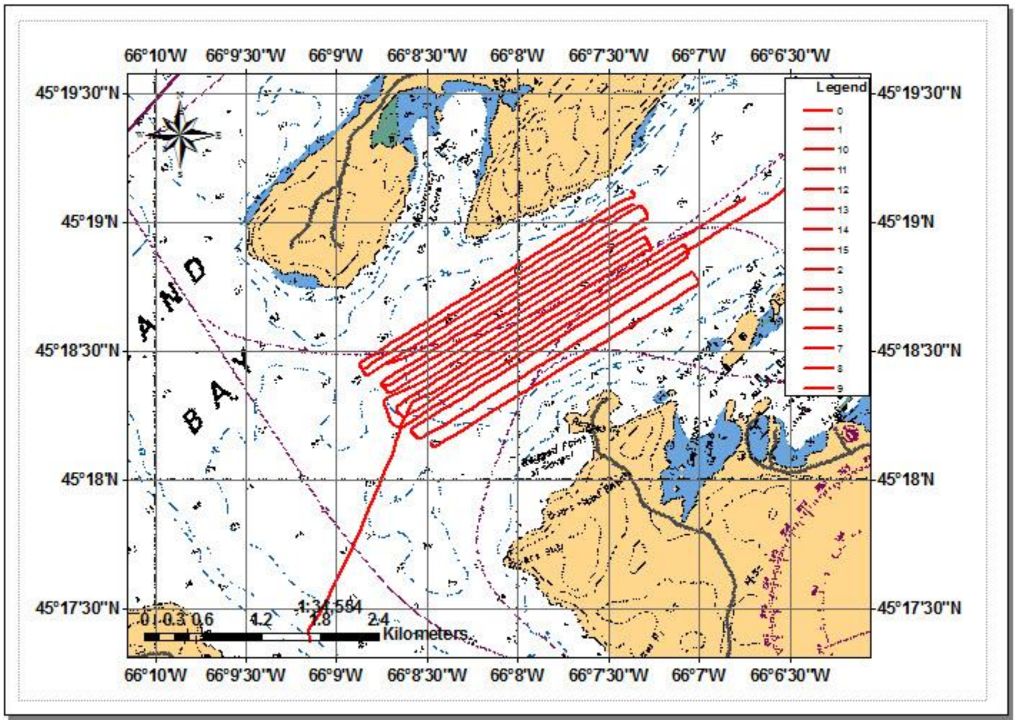

Figure 19: Oct. 2010 survey. 16 lines

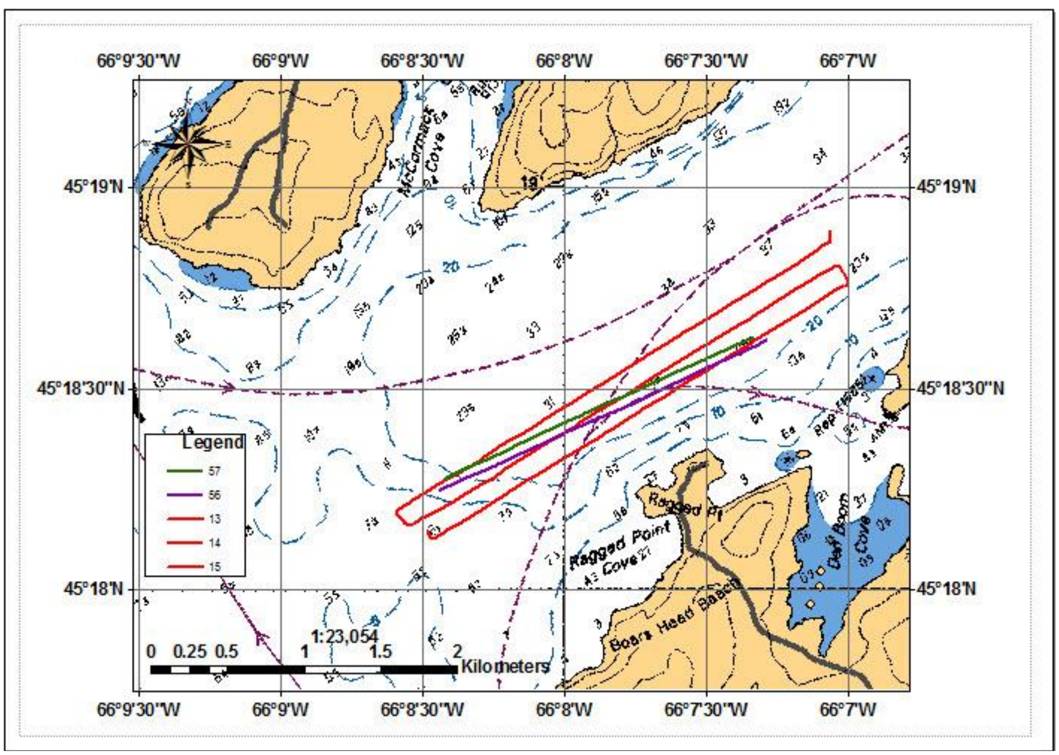

Figure 20: June and October survey crossing lines.

To locate the plumes, the Water column tool in Swathed software was used to find the coordinates of the ship at the time we saw the bubbles n the water column.

Steps:

1. From the vertical profile for the line, the gas plumes were located. The gas bubbles were vertical before the red line, which implies stagnant water with no current, while after the red line it is tilted which implies current flow.

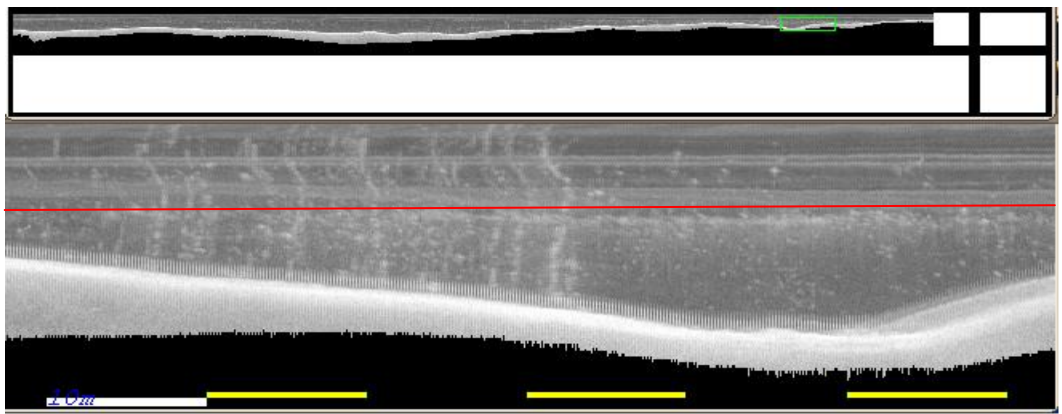

Figure 21: Vertical profile (upper) subset showing the gas plumes (lower) coming up straight and then tilting

2. Open the line (merged) in Swathed and use the Water Column tool to make sure that what we have seen in the vertical profile is gas bubbles.

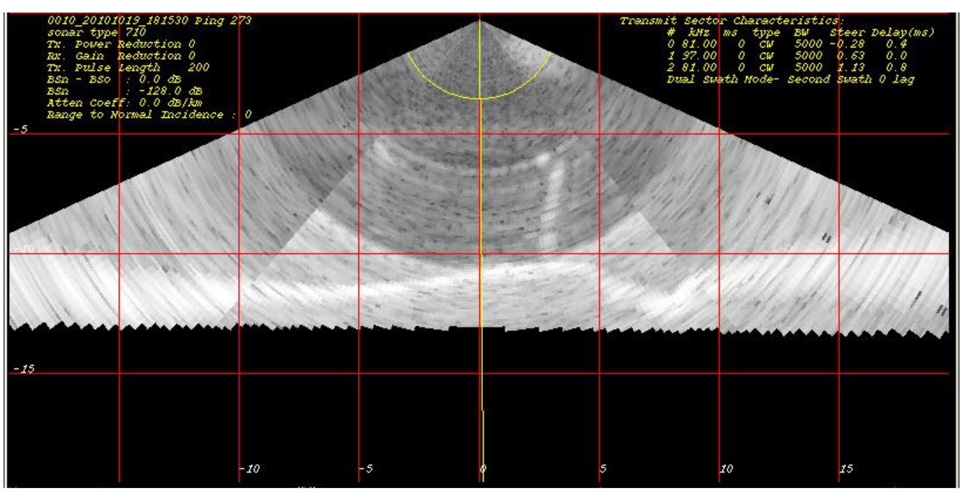

Figure 22: Water Column tool showing bubbles coming out of the seabed

3. The last step is to find the coordinates of the ship at the time of seeing the gas plume by using the list in swathed software.

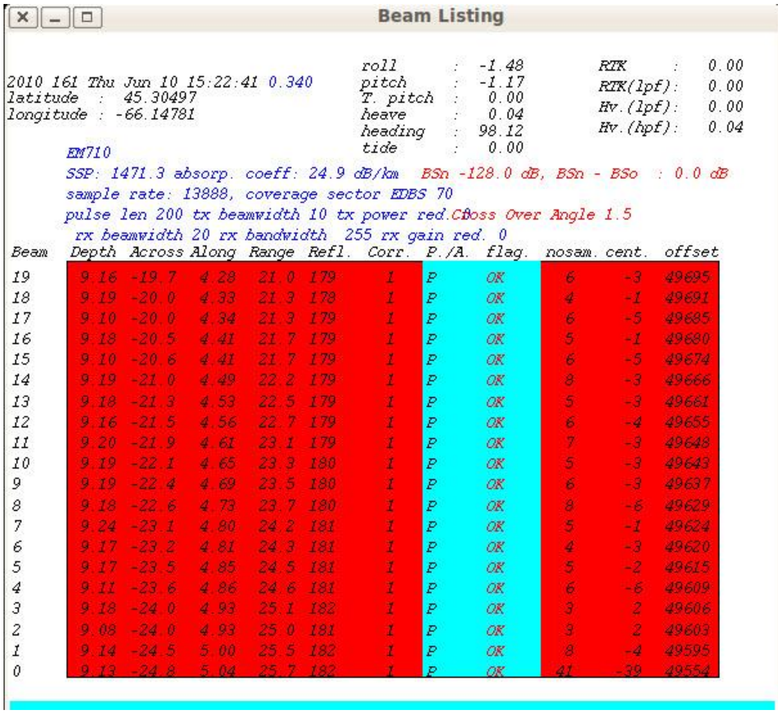

Beam Listing

2010 161 Thu Jun 10 15:22:41 0.340
latitude : 45.30497
longitude : -66.14781

roll : -1.48
pitch : -1.17
T. pitch : 0.00
heave : 0.04
heading : 98.12
tide : 0.00

RTK : 0.00
RTK(lpf): 0.00
Hv.(lpf): 0.00
Hv.(hpf): 0.04

EM710
SSP: 1471.3 absorp. coeff: 24.9 dB/km BSn -128.0 dB, BSn - BSo : 0.0 dB
sample rate: 13888, coverage sector EDBS 70
pulse len 200 tx beamwidth 10 tx power red.Cross Over Angle 1.5
rx beamwidth 20 rx bandwidth 255 rx gain red. 0

Beam	Depth	Across	Along	Range	Refl.	Corr.	P./A.	flag.	nosam.	cent.	offset
19	9.16	-19.7	4.28	21.0	179	1	P	OK	6	-3	49695
18	9.19	-20.0	4.33	21.3	178	1	P	OK	4	-1	49691
17	9.10	-20.0	4.34	21.3	179	1	P	OK	6	-5	49685
16	9.18	-20.5	4.41	21.7	179	1	P	OK	5	-1	49680
15	9.10	-20.6	4.41	21.7	179	1	P	OK	6	-5	49674
14	9.19	-21.0	4.49	22.2	179	1	P	OK	8	-3	49666
13	9.18	-21.3	4.53	22.5	179	1	P	OK	5	-3	49661
12	9.16	-21.5	4.56	22.7	179	1	P	OK	6	-4	49655
11	9.20	-21.9	4.61	23.1	179	1	P	OK	7	-3	49648
10	9.19	-22.1	4.65	23.3	180	1	P	OK	5	-3	49643
9	9.19	-22.4	4.69	23.5	180	1	P	OK	6	-3	49637
8	9.18	-22.6	4.73	23.7	180	1	P	OK	8	-6	49629
7	9.24	-23.1	4.80	24.2	181	1	P	OK	5	-1	49624
6	9.17	-23.2	4.81	24.3	181	1	P	OK	4	-3	49620
5	9.17	-23.5	4.85	24.5	181	1	P	OK	5	-2	49615
4	9.11	-23.6	4.86	24.6	181	1	P	OK	6	-6	49609
3	9.18	-24.0	4.93	25.1	182	1	P	OK	3	2	49606
2	9.08	-24.0	4.93	25.0	181	1	P	OK	3	2	49603
1	9.14	-24.5	5.00	25.5	182	1	P	OK	8	-4	49595
0	9.13	-24.8	5.04	25.7	182	1	P	OK	41	-39	49554

Figure 23: List in Swathed

This list will be good in case the plumes are at the center (Nadir) under the ship, but sometimes the plumes are seen under port side or starboard side of the ship.

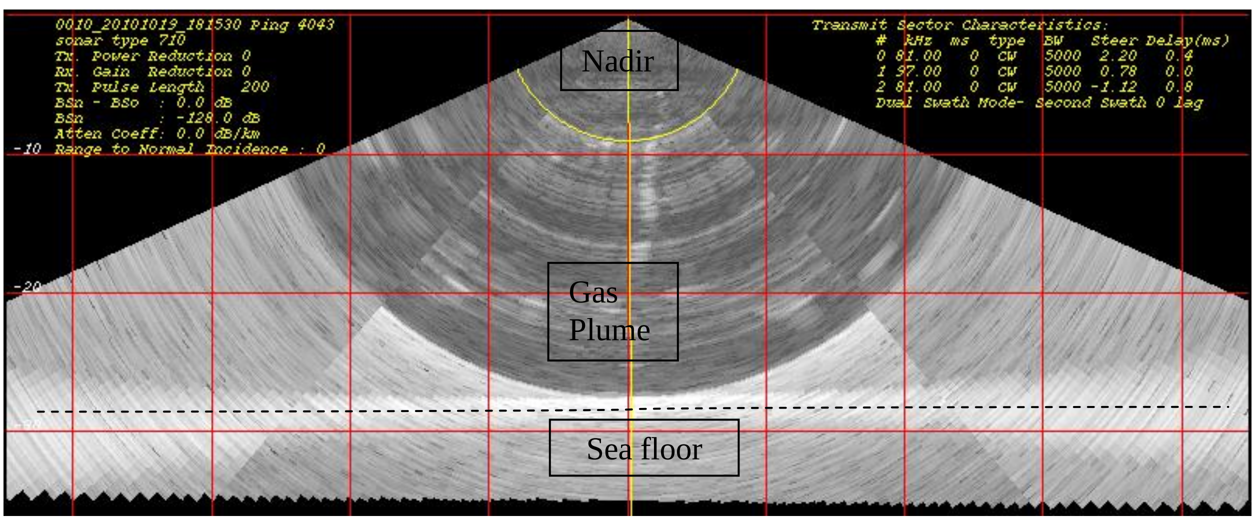

Figure 24: Gas plume at Nadir

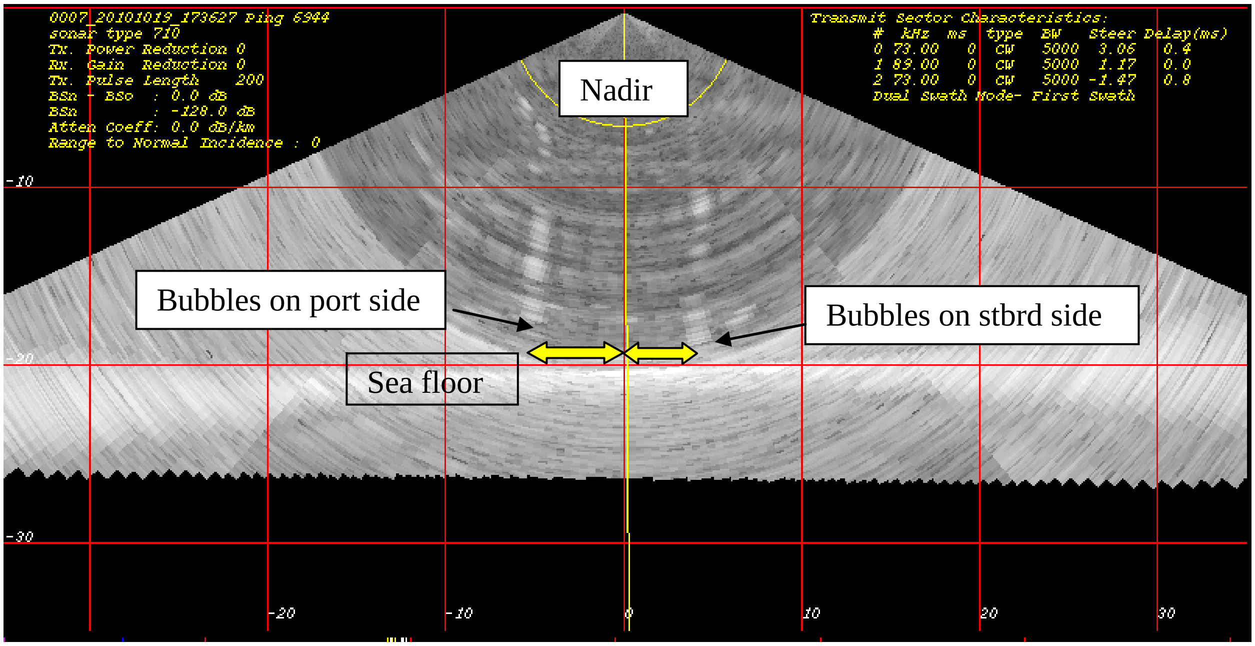

Figure 25: Bubbles on port side and stbrd side of the ship. Yellow arrows represent the distance from Nadir to plumes

Simplifying assumptions in positioning the plumes: there are 2 cases

1st case: If the gas bubbles are at Nadir, therefore the lat and long of reference point for ping can be used as the position of the gas plume.

2nd case: If the bubbles are at port side or starboard side of the ship

- Find the distance from Nadir by clicking on the plumes using the middle mouse button, and Swathed will give the exact across distance.
- Find the heading of the ship from the beam listing.
- Add 90° to ship's heading if the plumes are on the port side or subtract 90° from ship's heading if plumes are on the strbrd side.

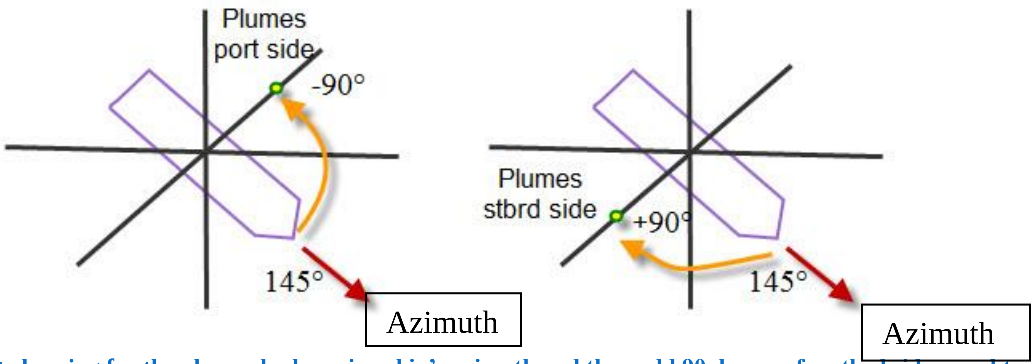

Figure 26: Calculate bearing for the plumes by knowing ship's azimuth and then add 90 degrees for stbrd side or subtract 90 degrees for port side plumes

- Add the result of range and bearing to the lat and long of the ship to get the exact position of the plumes using the following equation:

$lat2 = asin(sin(lat1)*cos(d/R) + cos(lat1)*sin(d/R)*cos(\theta))$

$lon2 = lon1 + atan2(sin(\theta)*sin(d/R)*cos(lat1), cos(d/R)-sin(lat1)*sin(lat2))$

θ is the bearing (in radians, clockwise from north); d/R is the angular distance (in radians), where d is the distance travelled and R is the earth's radius.

Comparing the results of June and October surveys:

To compare between the results of the two surveys, ArcGIS software was used to show the places of the gas plumes in the two surveys and then compare them together.

Survey lines in October were not parallel to survey lines in June but still very obvious that plumes were much denser in June than October.

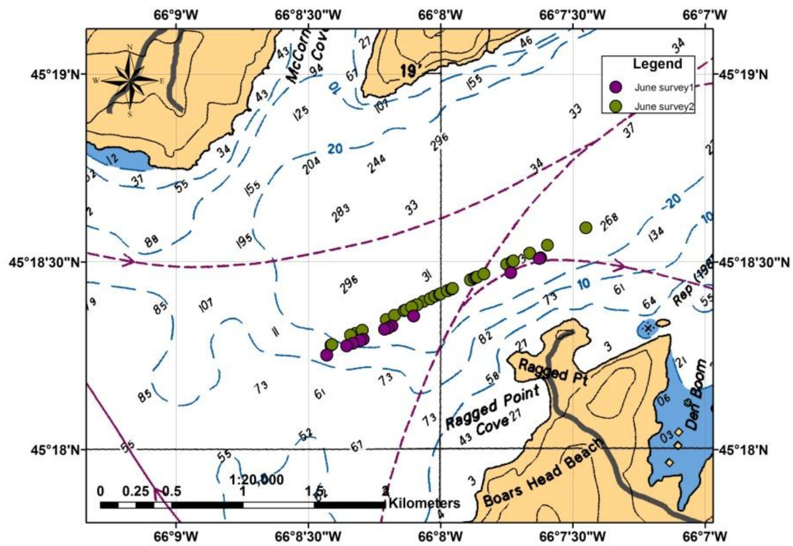

Figure 27: June survey – gas plumes

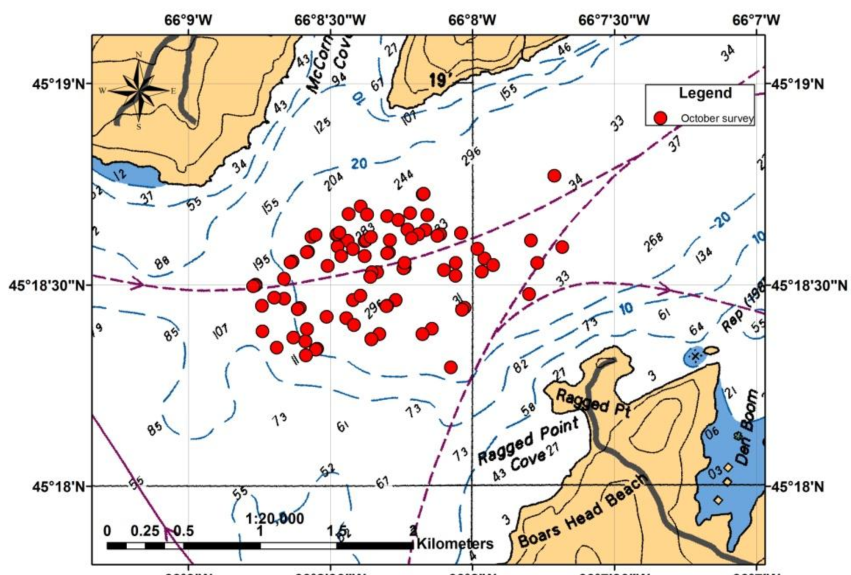

Figure 28: October survey- gas plumes

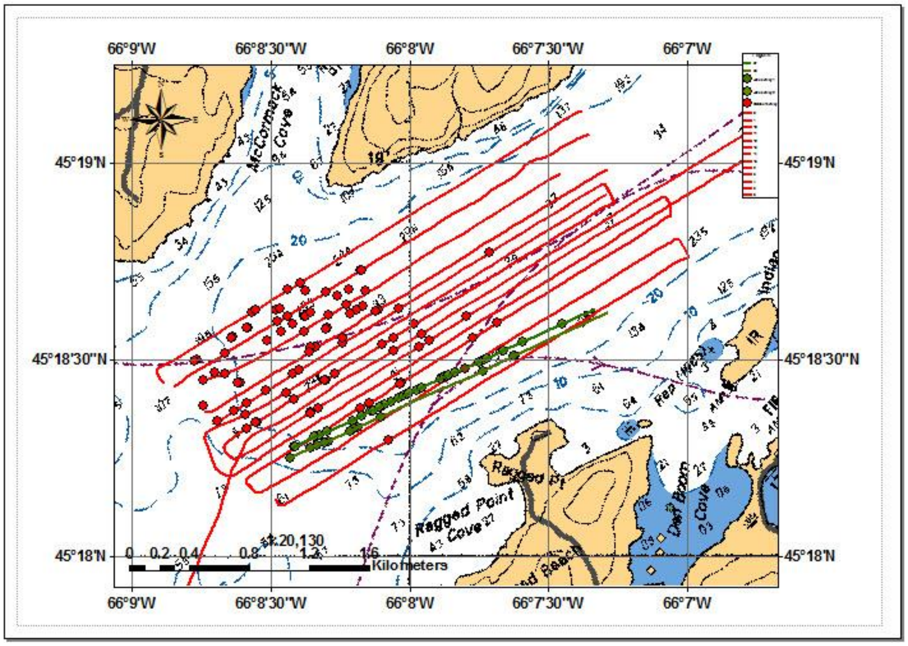

Figure 29: June and October surveys lines, gas plumes seem more dense in June.

5. Conclusion:

The gas plumes were seen only in certain areas, and can't be seen in any other part of the Kennebecasis Bay.

When there is high tide at the Bay of Fundy, salt water flows upstream into the river passing the Sill at the Reversing Falls, and will be trapped at the Gorge between the 2 Sills. According to Trites 1959, this Gorge acts as a mixing bowl, therefore, the fresh water of the river will mix with the salt water of the Bay of Fundy, which will decrease the salinity from 32ppt to about 24ppt. A portion of this water will continue up stream across the Grand Bay Sill going towards the Westfield Channel, and the other portion will across the Sill towards the Kennebecasis Bay and then will be divided again into salt water which will be take place in the middle layer of the channel between the old cold stagnant salt water (lower layer) and worm fresh water (upper layer), and saltier water which will go down to bottom of the basin with the old cold stagnant salt water.

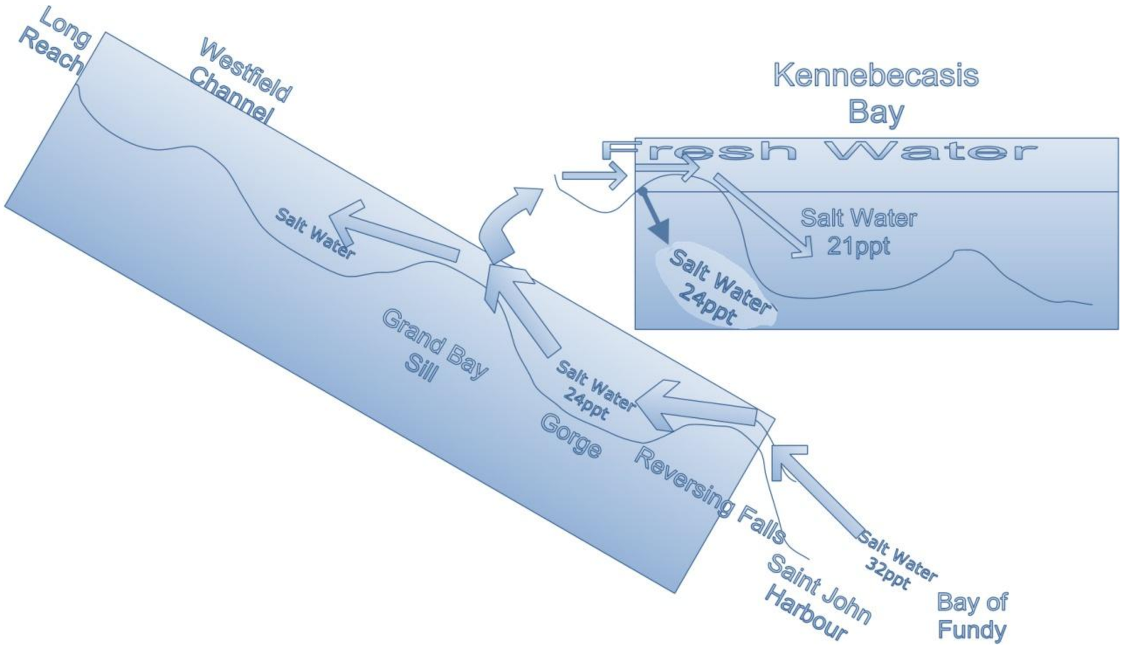

Figure 30: Flow of salt water from Bay of Fundy upstream Saint John River to Kennebecasis Bay

Hypotheses:

The saltier water which is injected into the lower layer of Kennebecasis Bay will renew the stagnant salt water in the basin, and increase oxygen level in this layer. When oxygen level increases, this will make bacteria active again and will start decomposing the organic materials such as algae and sea weed which came with the salt water from the Bay of Fundy to the Kennebecasis Bay and stayed at the bottom of the basin.

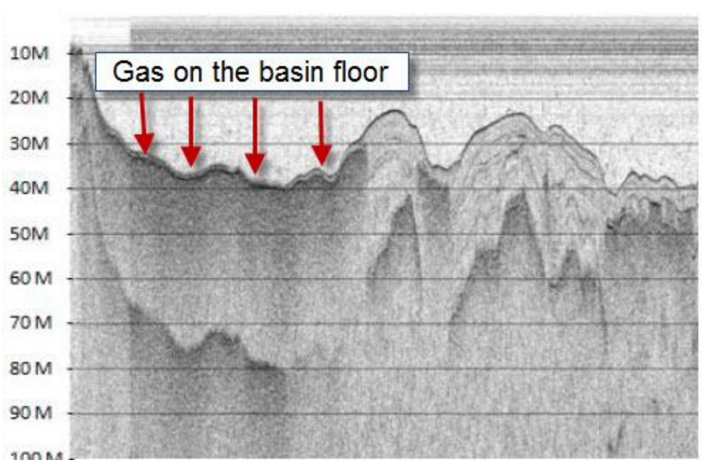

Figure 31: Gas on the basin floor of the Kennebcasis Bay

There are many gas plumes that the water column has detected, but there is a limit where it is practical to identify the plumes. The concentration was only on the major or big plumes. ArcGIS image (Figure 29), shows that there is no overlap between the plumes that was detected in both surveys, which leave us with one of two conclusions, either the plumes are moving from one place to another, or it can be active due to certain circumstances, and inactive when these circumstances change.

6. Appendix

Table for the lines with the pings in each line where we can see the gas plumes and the location of the gas plumes (lat and long)

Line #	Ping	Lat	Long
57	69	-66.1402	45.30464
57	648	-66.139	45.30508
57	1445	-66.1367	45.30576
57	4098	-66.1287	45.30837
57	97	-66.1402	45.30466
57	754	-66.1387	45.30515
57	644	-66.139	45.30507
57	916	-66.1383	45.30528
57	1444	-66.1367	45.30576
57	1632	-66.1362	45.30596
57	1843	-66.1356	45.30615
57	1889	-66.1355	45.30619
57	2050	-66.1351	45.30636
57	2268	-66.1344	45.30657
57	2127	-66.1348	45.30643
57	2010	-66.1352	45.30632
57	2408	-66.134	45.3067
57	2510	-66.1337	45.3068
57	2604	-66.1334	45.30689
57	2628	-66.1333	45.30691
57	2775	-66.1329	45.30705
57	2859	-66.1326	45.30713
57	2880	-66.1326	45.30715
57	3267	-66.1314	45.30755
57	3247	-66.1314	45.30753
57	3325	-66.1312	45.30761
57	3360	-66.1311	45.30764
57	3383	-66.131	45.30766
57	3513	-66.1306	45.30779
57	3963	-66.1292	45.30822
57	4069	-66.1288	45.30834
57	4098	-66.1287	45.30837
57	4415	-66.1277	45.30871
57	4760	-66.1266	45.30907
57	5523	-66.1242	45.30984
56	1669	-66.127	45.30851
56	1692	-66.1271	45.30848
56	2190	-66.1289	45.30785
56	3982	-66.135	45.30592

56	4465	-66.1364	45.30548
56	4547	-66.1366	45.3054
	4627	-66.1369	45.30533
	5129	-66.1382	45.30489
	5206	-66.1384	45.30484
	5400	-66.1389	45.30471
	5581	-66.1393	45.3046
	6319	-66.1405	45.30419
	19199	-66.1326	45.30942
	18787	-66.1343	45.30871
	3764	-66.1407	45.30695
	2893	-66.1432	45.306
00	3049	-66.1352	45.31043
00	3086	-66.1354	45.31037
02	4029	-66.1389	45.30885
02	4118	-66.1392	45.30885
03	4143	-66.1393	45.30866
03	609	-66.1444	45.30776
	2187	-66.1397	45.30953
	2583	-66.1382	45.31019
04	2844	-66.1372	45.31063
	7699	-66.1444	45.30858
	6044	-66.1407	45.31016
	5115	-66.1383	45.31117
05	4407	-66.1363	45.31208
	4387	-66.1362	45.31211
	6276	-66.1413	45.30992
	3915	-66.1428	45.31031
	4040	-66.1425	45.31041
	5230	-66.1399	45.31158
06	4945	-66.1406	45.31127
	6180	-66.1395	45.31125
	6198	-66.136	45.31123
	6956	-66.1413	45.31041
07	6944	-66.1413	45.31043
	6872	-66.1411	45.3105
	7790	-66.143	45.3097
	7816	-66.1431	45.30968
	8216	-66.1439	45.3093
	8270	-66.144	45.30926
	9430	-66.1461	45.30834
	9450	-66.1461	45.30832
	9520	-66.1462	45.30827
	1075	-66.1457	45.30747
	1665	-66.145	

	3305		45.3078
08	3645	-66.141	45.30912
	3907	-66.1403	45.30952
	4178	-66.1397	45.30982
	4212	-66.1396	45.31014
	4330	-66.1393	45.31018
	4932	-66.1377	45.31031
	5165	-66.137	45.31102
	4936	-66.1361	45.3113
	5075	-66.1365	45.3106
	5213	-66.1369	45.31043
9	5700	-66.1383	45.31026
	5734	-66.1383	45.30967
	7995	-66.1435	45.30964
	8054	-66.1436	45.30737
	9604	-66.1457	45.30733
	273	-66.1448	45.30641
	975	-66.1438	45.30573
	1470	-66.1431	45.30615
10	2067	-66.1419	45.3065
	2720	-66.1403	45.30701
	2886	-66.1399	45.30771
	3855	-66.1373	45.30789
	3833	-66.1374	45.30904
	4997	-66.134	45.30901
	6634	-66.1285	45.31047
	3377	-66.133	45.31285
	3814	-66.1343	45.30983
	4052	-66.135	45.30924
11	5055	-66.1378	45.30895
	5243	-66.1384	45.30771
	5257	-66.1384	45.30747
	5952	-66.1403	45.30745
	7016	-66.1425	45.30667
	7059	-66.1425	45.30569
	7449	-66.1431	45.30566
	2995	-66.1393	45.30542
	3174	-66.1388	45.30609
	2988	-66.1393	45.3063
12	5324	-66.1328	45.30608
	5546	-66.1321	45.30887
	6260	-66.1299	45.30915
	3340	-66.1281	45.31017
	3804	-66.1373	45.30989

	3802	-66.1295	45.30924
13	5222	-66.1338	45.30924
	5274	-66.1339	45.30738
	5906	-66.1357	45.30731
	6100	-66.1363	45.30651
14	6740	-66.1352	45.3063
15	6340	-66.1346	45.30795

7. References:

Chapter 1

- *G. K. Westbrook, Kate E. Thatcher, Eelco J. Rohling, Alexander M. Piotrowski, Heiko Palike, Anne H. Osborne, Euan G. Nisbet, Tim A. Minshull, Mathias Lanoiselle, Rachael H. James,Veit Huhnerbach, Darryl Green, Rebecca E. Fisher, Anya J. Crocker, Anne Chabert, Clara Bolton, Agnieszka Beszczynska-Moller, Christian Berndt, and Alfred Aquilina (2009), Escape of methane gas from the seabed along the West Spitsbergen continental margin, Geophysical Research Letters, VOL. 36, L15608, doi:10.1029/2009GL039191*
- *I. Leifer and R. J. Petro, The bubble mechanism for methane transport from the shallow sea bed to the surface: A review and sensitivity study, Cont. Shelf Res. 22, 2409-2428.*
- *I. Leifer , J.R. Boles, B.P. Luyendyk, and J.F. Clark (2004),Transient discharge from marine hydrocarbod seeps: spatial and temporal variability, Environmental Geology, 46: 1038 - 1052*
- *Kristen Schmidt (2004),Gas hydrate and methane plumes at Hydrate Ridge,* http://www.mbari.org/education/internship/04interns/04papers/Kristen_Schmidt04.pdf
- *World Ocean Review ,Climate change and methane hydrates,* http://worldoceanreview.com/en/ocean-chemistry/climate-change-and-methane-hydrates/
- *Peter G. Brewer, Edward T. Peltzer, Gernot Frederich , and Gregor Rehder (2002), Experimental determination of the fate of rising CO2 droplets in seawater, Environ. Sci. Technol. 2002, 36, 5441-5446.*
- *Peter G. Brewer, Baixin Chen, Robert Warzinki, Arthur Baggeroer, Edward T. Peltzer, Rachel M. Dunk, and Peter Walz (2006), Three-dimensional acoustic monitoring and modeling of a deep-sea CO2 droplet cloud, Geophysical research letters, VOL. 33, L23607, doi: 10.1029/2006GL027181.*
- *Water and Environmental Research Center (2010), Methane Gas seeps,* http://ine.uaf.edu/werc/people/katey-walter-anthony/methane-gas-seeps

Chapter 2

- *Mayer, L.A., Weber, T., Gardner, J. V., Malik, M., Doucet, M., Beaudoin, J. (2010), More than the bottom: Multibeam sonars and water - column imaging, American Geophysical Union, Fall Meeting 2010, abstract #OS12B-01*
- *J. H. Clarke (2006), Applications of mulitbeam water column imaging for hydrographic survey.*
- *EM 710 Multibeam echo sounder product description – Kongsberg.*

Chapter 3

- *R. W. Trites, 1960, An Oceanographical and Biological Reconnaissance of Kennebecasis Bay and the Saint John River Estuary, Jornal Fisheries Research Board of Canada, VOL.17, NO.3.*
- *J.E. Hughes Clarke and S.P. Haigh, 2005. Observation and interpretation of mixing and exchange over a sill at the mouth of the Saint John River estuary, conference Proceedings.*

- *S. Haigh and J. E. Clarke, Numerical modeling of Kennebecasis bay, conference Proceedings.*

- *P. J. Dickinson, 2008, Geomorphological processes and the development of the lower Saint John river human landscape, dissertation for Doctorate of Philosophy in the Graduate Academic Unit of Geology, University of New Brunswick.*

- *Nicole Delpeche,2007, Observations of advection and turbulent interfacial mixing in the Saint John River estuary, Phd thesis, Geodesy and Geomatics Engineering, University of New Brunswick.*